DT Assisted Task Offloading for C-V2X Networks With Imperfect DT Prediction Conditions

Fan, Bo; Xu, Zhenlin; Li, Zhidu; Wu, Yuan; Zhang, Yan

DOI
10.1109/TITS.2025.3549111

Publication date
2025

Document Version
Final published version

Published in
IEEE Transactions on Intelligent Transportation Systems

DT Assisted Task Offloading for C-V2X Networks With Imperfect DT Prediction Conditions

Bo Fan, Zhenlin Xu, Zhidu Li, *Senior Member, IEEE*, Yuan Wu, *Senior Member, IEEE*, and Yan Zhang, *Fellow, IEEE*

***Abstract*— The development of intelligent transportation has generated many ultra reliable low latency communication (URLLC) tasks, which require sufficient communication and computation resources for task offloading and processing. Although mobile edge computing (MEC) provides a promising solution, its efficiency is subject to the limited knowledge and analysis capability on the physical networks. Therefore, in this paper, we propose a digital twin (DT) empowered MEC framework to strengthen the MEC task offloading efficiency in cellular vehicle-to-everything (C-V2X) networks. Our proposed DT is constructed through a hybrid data-driven and model-driven approach to capture the realistic transportation network features. Then, DT leverages the metric of time to collision to predict vehicular safety levels and estimates the corresponding URLLC task requirements of future time slots. The prediction results are further utilized to make decisions on the URLLC resource reservation. Different from conventional studies, we consider the influence of DT's inaccurate predictions (i.e., the prediction with error) on the resource allocations. Specifically, the inaccurate DT prediction results are considered as uncertain constraints of the resource reservation problem. A robust parameter from the robust optimization is adopted to adjust the tradeoff between the problem uncertainty and solution optimality degree. Further, we leverage the optimized resource reservation results to construct the task offloading problem. The problem is decoupled into two sub-problems of channel resource allocation and computation resource allocation, respectively. And a two-stage matching algorithm is developed to solve each sub-problem based on the resource reservation constraints. Finally, realistic road information is mapped into DT for simulations. Simulation results validate the advantages of our proposed approach by comparing with existing schemes.**

***Index Terms*— Digital twin, mobile edge computing, C-V2X networks, vehicular safety prediction, robust optimization.**

Received 5 March 2024; revised 28 July 2024 and 18 January 2025; accepted 1 March 2025. This work was supported in part by the Urban Carbon Neutrality and Urban Renewal Science and Technology Innovation Fund, Beijing University of Technology; and in part by the Science and Technology Development Fund of Macau SAR under Grant FDCT 0158/2022/A and Grant MYRGGRG2023-00083-IOTSC-UMDF. The Associate Editor for this article was S. Kumari. *(Corresponding author: Zhidu Li.)*

Bo Fan is with Beijing Key Laboratory of Traffic Engineering, College of Metropolitan Transportation, Beijing University of Technology, Beijing 100124, China (e-mail: fanbo@bjut.edu.cn).

Zhenlin Xu is with the Department of Transport and Planning, Faculty of Civil Engineering and Geosciences, Delft University of Technology, 2628 CD Delft, The Netherlands (e-mail: z.xu-28@student.tudelft.nl).

Zhidu Li is with the School of Communications and Information Engineering, Chongqing University of Posts and Telecommunications, Chongqing 400065, China (e-mail: lizd@cqupt.edu.cn).

Yuan Wu is with the State Key Laboratory of Internet of Things for Smart City, University of Macau, Macau SAR, China (e-mail: yuanwu@um.edu.mo).

Yan Zhang is with the Department of Informatics, University of Oslo, 0313 Oslo, Norway, and also with the Simula Metropolitan Center for Digital Engineering, 0164 Oslo, Norway (e-mail: yanzhang@ieee.org).

Digital Object Identifier 10.1109/TITS.2025.3549111

I. Introduction

CELLULAR Vehicle-to-Everything (C-V2X) is a key enabler to support future intelligent transportation applications such as safety driving, intelligent cruise and vehicular infotainment, etc [1], [2], [3]. These applications can be categorized into two types, i.e., the ultra reliable low latency communication (URLLC) application and the non-URLLC application. Specifically, the URLLC applications are related with traffic safety, which require up to 1 ms delay tolerance and 99.99% reliability [4], [5]. Therefore, how to effectively reduce the packet transmission latency and packet loss has become the most challenging issue for the C-V2X networks.

A promising solution is to offload the application tasks generated in the C-V2X networks to roadside units via mobile edge computing (MEC) for reducing the task-execution latency and improving reliability. The existing MEC task offloading schemes mainly focus on some specific scenarios (e.g., collaborative driving [6], vehicular platoon [7] and vehicular infotainment [8], [9], etc) with homogeneous application types. However, in many practical cases, the URLLC and the non-URLLC applications will be simultaneously generated and the existence of the non-URLLC applications will occupy the resources which are available for the URLLC applications. Therefore, it is vital to guarantee the performance of the URLLC applications under hybrid application scenarios. Moreover, the dynamic and decentralized topology of the C-V2X networks also increases the task offloading complexity, which can lead to inefficient task offloading decisions.

To cope with the above concerns, our idea is to enable the prediction of the incoming URLLC tasks and thus make resource reservations in advance to guarantee efficient task offloading. To achieve this, digital twin (DT), which is an emerging technology for intelligent industry [10], provides a promising solution. DT is defined as a virtual representation to reflect the real-time digital counterpart of a physical object or process. It was initially introduced to solve the product life-cycle management problem in aerospace and automotive industries [11]. A DT object mainly includes three elements, namely, a physical object in physical layer, a digital object in virtual layer and the data link between the two layers [12].

In our paper, DT is adopted to collect the physical network data and analyze the network conditions by combining the data with its internal simulators. The analysis results can help predict the future URLLC application requirements, which enables the network controller to make resource reservation and allocation decisions in advance for ensuring the URLLC service quality. In addition, we also consider the inaccuracy incurred by DT's data collection and analysis error, which will result in inefficient network control decisions. To the best of the authors' knowledge, few studies have investigated the optimization performance under imperfect DT analysis conditions. The main contributions are summarized as follows.

- We propose a DT empowered MEC framework for C-V2X communications. The proposed framework consists of two domains, i.e., the physical domain and the DT domain. In the physical domain, the application tasks generated by the smart vehicles can be offloaded to the computation units at the roadside unit (RSU) for reducing the processing latency. The DT domain collects physical network data and combines these data with Simulation of Urban Mobility, i.e., SUMO,[1] for simulating and predicting the transportation network conditions. Specifically, a metric of time to collision is introduced to predict vehicular safety conditions and to further estimate the requests of RSU assisted vehicular safety control tasks (typical URLLC tasks). The prediction and estimation results are utilized to reserve and pre-allocate the channel and computing resources for the URLLC tasks.
- The DT empowered resource allocation for the task offloading is considered in the following two stages. In the first stage, we investigate the DT domain's resource reservation problem. The problem is formulated under inaccurate channel and computation resource prediction constraints, and robust optimization is introduced to solve it. The problem can be decoupled into two parallel sub-problems. Then, a robust parameter is adopted to adjust the conservatism of uncertain constraints, i.e., the tradeoff between the problem constraint uncertainty and solution optimality degree. The problem constraint uncertainty is represented by the number of DT's inaccurate predictions which can be handled by the robust parameter. The optimized solutions of the resource reservation problem under the given robust parameter can be output from the DT domain to the physical domain, which help determine the task offloading decisions more efficiently.
- In the second stage, we investigate the physical domain's task offloading problem, which is formulated under the resource reservation constraints of the DT domain. To reduce the computational complexity, the problem is further decoupled into two sub-problems, i.e., the channel allocation problem and the computation resource allocation problem. In particular, we propose a two-step matching approach for the each sub-problem. Firstly, the URLLC tasks are considered in priority based on the resource reservation constraints. Secondly, we determine the resource allocation for the non-URLLC tasks.
- We map the realistic road structure, speed limitation and vehicular density of G2 Beijing-Shanghai Highway into SUMO for constructing the DT simulator and further predicting the URLLC task arrival time and requirements. Simulations compare the task delay of our proposed resource reservation and task offloading scheme with the existing benchmarks. We also evaluate the algorithm performance under different resource reservation numbers and prediction errors.

The remainder of this paper is organized as follows. Section II presents the literature review. In Section III, we present the DT empowered MEC framework for C-V2X networks. In Section IV, we present the problem formulation. In Section V, we present the robust optimization based solution for the resource reservation problem. In Section VI, we leverage matching theory to decouple and solve the task offloading problem. In Section VII, we evaluate the performance of the proposed scheme. Section VIII concludes this paper.

II. Literature Review

The paradigm of MEC has been regarded as an efficient solution for enabling various computation-intensive and latency-sensitive services in future wireless networks. In [14], Gao et al. investigated the delay and energy minimization for vehicular tasks and proposed a two-layer solution. The upper layer determined deep Q-network based task offloading scheduling, and the lower level determined the gradient descent based CPU frequency allocation. In [15], Nguyen et al. studied a collaborative task computing and offloading scheme to efficiently reduce the redundant data and utilize the idle resources in nearby MEC servers. In [16], Hou et al. developed a reliable task offloading scheme by jointly considering the partial offloading, reliability-oriented task allocation, and reprocessing mechanism, and then a particle swarm algorithm was applied for maximizing the reliability under the latency constraints. In [17], Wang et al. proposed a regional C-V2X network with dual MEC planes, in which MEC servers cooperated with each other for resource sharing. Deep reinforcement learning was adopted to minimize the offloading latency under the proposed network framework. In [18], Sun et al. introduced task replication to guarantee the task offloading delay and to suit the highly dynamic environment of V2X networks. Specifically, the optimal number of task replicas was derived and a learning-based task replication algorithm was further developed. In [19], Cui et al. proposed a multi-objective reinforcement learning strategy to reduce the total latency and improve the reliability of communication and computing resource allocations. In [20], Chen et al. formulated the computation offloading problem as a multi-agent Markov decision process and developed an online distributed reinforcement learning algorithm to solve the problem. In [21], Tian et al.conduct a three-tier hierarchical service system with multiple mobile users(UEs), multiple mobile edge computing servers(MECs), and a single cloud center (CC) proposed a user preference-based hierarchical

[1]SUMO is an open-source microscopic traffic simulator with high scalability and compatibility [13].

offloading strategy for collaborative cloud-edge computing, which utilizes a three-tier service system to optimize task offloading by considering user preferences and real-time task characteristics to reduce response time and energy consumption.

In addition, energy consumption [22], [23], information security [24], [25] and vehicle platoon applications [26] were also considered for optimization in the MEC enabled C-V2X networks. In [22], Ning et al. minimized the total energy consumption of RSUs via latency estimation and task scheduling. In [23], Zhai et al. formulated an energy-aware execution cost model to extend the running time of MEC enabled C-V2X networks, and a heuristic optimization algorithm was designed to solve the proposed problem. In [24], Bao et al. utilized federated learning to design a MEC-based joint client selection and networking scheme, and a fuzzy logic algorithm was used in the process of client selection considering the vehicle velocity, vehicle distribution, and the wireless link connectivity between vehicles. In [25], secure beamforming and artificial noise schemes were investigated to improve the ergodic secrecy rates of vehicular computation offloading. In [26], a mobile-edge-platooning cloud architecture was proposed to provide aggregated resources of computing, storage, communication with the aim of optimizing the overall transportation network efficiency.

Furthermore, early researches have shed light on the combination of MEC and DT for optimizing the C-V2X networks. In [27], a DT assisted real-time traffic data prediction method was proposed to address the traffic data sparsity and incompleteness under 5G-V2X communications. In [28], a DT enabled Vehicle-to-Cloud communication framework was designed to realize cooperative ramp merging, which allowed connected vehicles to cooperate with each other before arriving at the merging zone. In [29], Tan et al. deployed the consortium blockchain to track and secure the vehicular resource sharing among DT entities in the cloud. In [30], Zhao et al. introduced an intelligent DT based software-defined vehicular networking architecture for improving packet delivery ratio and reducing delay. In [31], Sun et al. investigated the task offloading problem in DT based edge networks and applied Lyapunov optimization for the long-term migration cost constraint simplification. In [32], Xu et al. analyzed the quality of service in the DT empowered C-V2X multi-user offloading system and applied deep Q-network to optimize the service offloading decisions. In [33], Cha et al. proposed a virtual edge formation algorithm to utilize spare computational resources of multiple vehicles as a virtual server, which showed advantages in computation offloading task completion ratio and execution time. In [34], Zhang et al. investigated a DT empowered content caching mechanism for social-aware vehicular edge networks, where DT was leveraged to model the social relations between vehicles and to understand the traffic flow distribution. In [35], a deep reinforcement learning based safety control decision was proposed under the DT empowered MEC framework to guarantee the transportation safety and efficiency.

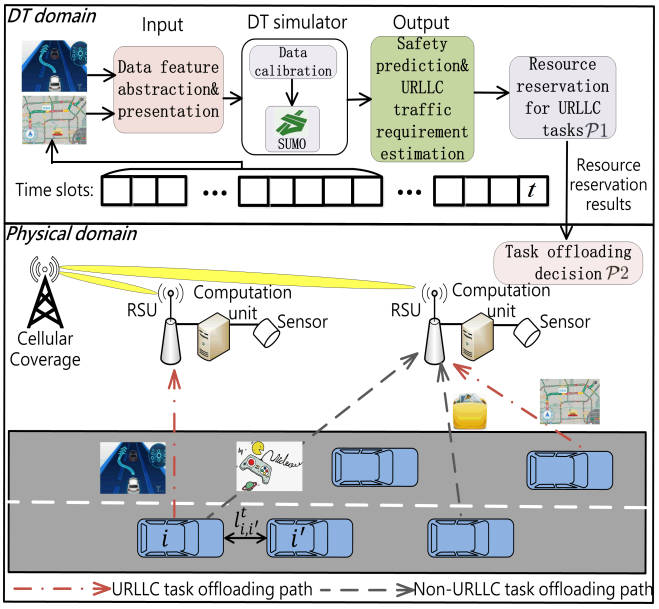

Fig. 1. The proposed DT empowered C-V2X network.

Significant as the aforementioned researches are, two important challenges remain unsolved. First, to the best of the authors' knowledge, few studies investigate on how DT can be leveraged to improve the URLLC performance, which is one of the most crucial tasks in C-V2X networks. In addition, there exists few studies accounting for the following issue, namely, the inaccuracy due to the DT's data collection and analysis error, which will degrade network control decisions.

III. DT Empowered C-V2X Network Framework

Our proposed DT empowered C-V2X network framework is presented in Fig. 1, which consists of the physical domain and the DT domain. Details are as follows.

A. Physical Domain

The physical domain is shown in the lower part of Fig. 1, where vehicles generate applications such as safety driving, intelligent navigation and vehicular infotainment, etc. Limited by insufficient on-board computing capability, the vehicles need to offload these tasks to the RSU. In addition, we consider that vehicles are located within the coverage of cellular base stations such that the vehicles can use the cellular channels to perform V2X communications. The computation unit and sensors are linked to the RSU through wired links. The computation unit runs artificial intelligence based algorithms to assist with the vehicular data processing and decision-making tasks. The roadside sensors collect and provide Non-Line-of-Sight (NLoS) environment data for vehicles, such as the average speed and density of the NLoS lane sectors. We consider two application task types, i.e., RSU-assisted vehicular safety control as the URLLC task and vehicular infotainment as the non-URLLC task.

B. DT Domain

The DT domain is shown in the upper part of Fig. 1, where the key features of the physical transportation and C-V2X networks can be simultaneously extracted, modeled and

maintained in a cloud-based platform. Note that the platform can be linked to the physical domain through wired backhauls. The DT can predict the transportation safety risks and the corresponding offloading requirements based on its simulation and analysis on the physical networks. The predicted results are leveraged by the physical domain to optimize the network task offloading decisions. Details as follows.

- **DT construction:** DT is constructed through a hybrid data-driven and model-driven method. The physical domain data (e.g., road map, infrastructure location, vehicle density, etc) can be collected and mapped to the DT domain through wired backhauls. DT utilizes these data to calibrate its internal simulators or models for capturing the realistic features of physical networks. For instance, DT can import realistic road maps, vehicle density and positions into SUMO. By combining the data feature with SUMO's road simulator and vehicle mobility modules, SUMO can simulate the transportation network and predict the vehicle trajectory, speed and traffic congestion or accidents within a certain range of the future time slots. The predicted results can be delivered to the physical domain for optimizing the transportation and C-V2X network control strategies.
- **Vehicular safety prediction:** We introduce time to collision (TTC), the classic transportation safety metric, to evaluate the vehicular safety. The predicted TTC of vehicle i at time slot t can be calculated as $\Pi_i^t = l_{i,i'}^t/(v_i^t - v_{i'}^t)$, where i' represents the neighboring vehicle in the directly front of i. v_i^t and $v_{i'}^t$ are the speeds of vehicles i and i', respectively. $l_{i,i'}^t$ is the distance between vehicles i and i' at time slot t. Note that these parameters can be predicted and obtained via the DT simulator. If $\Pi_i^t < \Pi_{threshold}$, the vehicular safety risk level is predicted to be high,[2] and safety control needs to be performed between the two vehicles. For instance, vehicle i performs the lane-changing to overtake vehicle i', or vehicle i decelerates to keep a safety distance. The safety control decision requires RSU assistance due to the following two reasons. First, compared to local vehicular decisions, the RSU sensor can provide NLoS road information and significantly improve the safety control efficiency. Second, RSU can support more efficient and intelligent decision-making strategies with more powerful computation capability.
- **URLLC task requirement estimation:** The aforementioned RSU assisted safety control decisions are typically URLLC tasks. Without loss of generality, we use the URLLC tasks to denote the RSU assisted safety control decision tasks in the paper. And we consider that DT can estimate the URLLC task requirement based on the vehicular safety prediction results as follows: $\mathcal{E}_{i,j}^t = \{\tilde{C}_{i,j}^t, \tilde{Q}_{i,j}^t | \Pi_i^t < \Pi_{threshold}\}, \forall j \in \mathcal{J}_{\text{UR}}$. $\tilde{C}_{i,j}^t$ and $\tilde{Q}_{i,j}^t$ denote the estimated channel number and computation resource number required by URLLC task j of vehicle i at time slot t, respectively. $\mathcal{J}_{\text{UR}}$ represents the URLLC task application set. Note that $\tilde{C}_{i,j}^t$ can be obtained by comparing the decision task complexity with the historical average V2X link rate of the coverage area. $\tilde{Q}_{i,j}^t$ can be obtained by comparing the decision task complexity with the RSU's computation speed per resource unit. The prediction and estimation results can be utilized by the physical network to reserve and pre-allocate resources for URLLC tasks.

The most challenging part of our proposed DT empowered C-V2X network resource allocation lies in the DT prediction and estimation accuracy. Although the DT simulator is based on real-world network data, it is impossible to achieve 100% accuracy due to such reasons as inadequate data sample, DT simulator deviation and DT estimation error, etc. When the predicted resource requirement is greater than the actual value, part of the reserved resources will be wasted. On the contrary, when the predicted resource requirement is smaller than the actual value, the URLLC tasks cannot be offloaded and completed within the given deadline. Therefore, in the following section, we will account for the inaccurate DT prediction condition and study the corresponding resource reservation and task offloading scheme.

IV. Problem Formulation under the Proposed Framework

The resource reservation problem leverages the DT prediction error to determine the resource reservation of URLLC tasks. The task offloading problem determines the communication and computation resource allocation based on the resource reservation results. For the sake of clarification, Table I presents the relevant variables for our proposed resource reservation and task offloading problems.

A. The Resource Reservation Problem in the DT Domain

Let $i \in \mathcal{I}$ denote the vehicle user, $j \in \mathcal{J}$ denote the application task, $k \in \mathcal{K}$ denote the RSU, $c \in \mathcal{C}$ denote the channel resource in the cellular resource pool and $q \in \mathcal{Q}_k$ denote the computation resource where $\mathcal{Q}_k$ is the computation resource set of RSU k. The application task set includes both URLLC tasks and non-URLLC tasks. Recall that $\mathcal{J}_{\text{UR}}$ represents the URLLC application task set, where $\mathcal{J}_{\text{UR}} \subseteq \mathcal{J}$, the remaining tasks constitute the non-URLLC task set. And we consider that DT's prediction results have errors $\widehat{C}_{i,j}^t$ and $\widehat{Q}_{i,j}^t$, compared to the actual values $C_{i,j}^t$ and $Q_{i,j}^t$. Hence we know that $\tilde{C}_{i,j}^t$ and $\tilde{Q}_{i,j}^t$ have uncertain values in the ranges of $\left[C_{i,j}^t - \widehat{C}_{i,j}^t, C_{i,j}^t + \widehat{C}_{i,j}^t\right]$ and $\left[Q_{i,j}^t - \widehat{Q}_{i,j}^t, Q_{i,j}^t + \widehat{Q}_{i,j}^t\right]$, respectively. To this end, at each time slot t, we can formulate the resource reservation problem in the DT domain as follows:

$$
\begin{aligned}
&\mathcal{P}1: \\
&\min \quad \sum_{i\in\mathcal{I}} \sum_{j\in\mathcal{J}_{\text{UR}}} \left(\epsilon_1 X_{i,j}^t + \epsilon_2 Y_{i,j}^t\right) \\
&\text{s.t.} \quad \text{C1}: \sum_{i\in\mathcal{I}} \sum_{j\in\mathcal{J}_{\text{UR}}} X_{i,j}^t \le |\mathcal{C}| \\
&\qquad\quad \text{C2}: \sum_{i\in\mathcal{I}} \sum_{j\in\mathcal{J}_{\text{UR}}} Y_{i,j}^t \le \sum_{k\in\mathcal{K}} |\mathcal{Q}_k|
\end{aligned}
$$

[2]Smaller Π_i^t means higher collision probability between vehicles i and i'. Note that only positive TTC value is meaningful.

TABLE I
SUMMARY OF KEY VARIABLES

variable	meaning
$\mathcal{I}$	vehicle set
$\mathcal{J}$	application task set
$\mathcal{K}$	RSU set
$\mathcal{C}$	channel set
$\mathcal{J}_{\text{UR}}$	URLLC application task set
$\tilde{C}^t_{i,j}$	estimated channel number required by URLLC task j of vehicle i at time slot t
$\tilde{Q}^t_{i,j}$	estimated computation resource number required by URLLC task j of vehicle i at time slot t
$C^t_{i,j}$	actual required channel number
$Q^t_{i,j}$	actual required computation resource number
$\widehat{C}^t_{i,j}$	estimation error of required channel number
$\widehat{Q}^t_{i,j}$	estimation error of required computation resource number
Ψ^1_i	channel resource allocation fairness index
Ψ^2_i	computation resource allocation fairness index
ϵ_1	reservation cost per channel resource
ϵ_2	reservation cost per computation resource
$X^t_{i,j}$	optimization variable of channel resource reservation
$Y^t_{i,j}$	optimization variable of computation resource reservation
$d^t_{i,j}$	task offloading delay
$\alpha^t_{i,j,k}$	RSU-vehicle association variable
$\beta^t_{i,j,c}$	optimization variable of channel resource allocation
$\gamma^t_{i,j,c}$	optimization variable of computation resource allocation
$S^t_{i,j}$	application task size
$R^t_{i,j,k,c}$	communication rate of vehicle i's application j to RSU k on channel c at time slot t
$W^t_{k,q}$	computation rate computation resource k of RSU q at time slot t
B	channel bandwidth
$p^t_{i,j,k,c}$	transmit power of vehicle i's application j to RSU k on channel c at time slot t
$g^t_{i,j,k,c}$	channel gain of vehicle i's application j to RSU k on channel c at time slot t
N_0	white Gaussian noise power
I_{cell}	cell-to-vehicle co-channel interference
Γ_i	robust parameter
$\tilde{A}^t_{i,j}$	equivalent uncertain constraint parameters of C3
$\tilde{B}^t_{i,j}$	equivalent uncertain constraint parameters of C4
$\mathcal{U}_i$	vehicle i's task set with uncertain communication demand
$Z^t_{i,j}$, $U^t_{i,j}$	temporary variables for problem transformation

$$\text{C3}: \sum_{j\in\mathcal{J}_{\text{UR}}} X^t_{i,j}/\tilde{C}^t_{i,j} \geq \Psi^1_i, \quad \forall i \in \mathcal{I}$$
$$\text{C4}: \sum_{j\in\mathcal{J}_{\text{UR}}} Y^t_{i,j}/\tilde{Q}^t_{i,j} \geq \Psi^2_i, \quad \forall i \in \mathcal{I}$$

$$\text{variables}: \quad X^t_{i,j} \in \mathbb{N}, \quad \forall i \in \mathcal{I}, j \in \mathcal{J}_{\text{UR}}$$
$$Y^t_{i,j} \in \mathbb{N}, \quad \forall i \in \mathcal{I}, j \in \mathcal{J}_{\text{UR}} \tag{1}$$

The objective of problem $\mathcal{P}1$ aims to minimize the total resource reservation cost. The decision variables $X^t_{i,j}$ and $Y^t_{i,j}$ denote the amount of reserved channels and computation resources, with ϵ_1 and ϵ_2 representing the reservation cost per channel and computation resource, respectively. $\mathbb{N}$ denotes the non-negative integer set. Constraint C1 restricts that the maximum number of reserved channels cannot exceed the total channel resource number $|\mathcal{C}|$. Constraint C2 guarantees that the maximum number of reserved computation resources on each RSU cannot exceed the total computation resource number $|\mathcal{Q}_k|$. Constraints C3 and C4 guarantee the minimum amount of reserved channel and computation resources to guarantee the allocation fairness among different URLLC application tasks. Ψ^1_i and Ψ^2_i are the allocation fairness indexes of the communication and computation resources, respectively.

1) Problem Uncertainty Analysis: Different from conventional integer programming problems, the non-deterministic parameters $\tilde{C}^t_{i,j}$ and $\tilde{Q}^t_{i,j}$ in constraints C3 and C4 are subject to uncertainty ranges of $\left[C^t_{i,j} - \widehat{C}^t_{i,j}, C^t_{i,j} + \widehat{C}^t_{i,j}\right]$ and $\left[Q^t_{i,j} - \widehat{Q}^t_{i,j}, Q^t_{i,j} + \widehat{Q}^t_{i,j}\right]$. Therefore, constraints C3 and C4 make problem $\mathcal{P}1$ highly-complex and intractable. Notice that, as a special yet very ideal situation, the DT's prediction results can be accurate and certain without errors, and there exists $\widehat{C}^t_{i,j} = \widehat{Q}^t_{i,j} = 0$. In this special case, C3 and C4 are deterministic constraints. And problem $\mathcal{P}1$ converts to a conventional integer programming problem, which can be solved by conventional solvers. In our study, we consider the realistic situation where the DT's prediction results are partly inaccurate. If the prediction result of vehicle i's task j is inaccurate, we have $\widehat{C}^t_{i,j} \neq 0$ and $\widehat{Q}^t_{i,j} \neq 0$.

B. The Task Offloading Problem in the Physical Domain

The optimized reservation results of $\mathcal{P}1$, i.e., $X^{t*}_{i,j}$ and $Y^{t*}_{i,j}$ are output to the physical domain to specify the constraints in the task offloading problem in the physical domain. Specifically, at each time slot t, the task offloading problem in the physical domain is formulated as follows:

$$\mathcal{P}2:$$
$$\min \quad \sum_{i\in\mathcal{I}}\sum_{j\in\mathcal{J}} d^t_{i,j}$$
$$\text{s.t.} \quad \text{D1}: \sum_{i\in\mathcal{I}}\sum_{j\in\mathcal{J}}\sum_{c\in\mathcal{C}} \alpha^t_{i,j,k}\beta^t_{i,j,c} \leq |\mathcal{C}|$$
$$\text{D2}: \sum_{i\in\mathcal{I}}\sum_{j\in\mathcal{J}}\sum_{q\in\mathcal{Q}_k} \alpha^t_{i,j,k}\gamma^t_{i,j,q} \leq |\mathcal{Q}_k|, \quad \forall k$$
$$\text{D3}: \sum_{k\in\mathcal{K}} \alpha^t_{i,j,k} \leq 1, \quad \forall i \in \mathcal{I}, j \in \mathcal{J}$$
$$\text{D4}: \sum_{i\in\mathcal{I}}\sum_{j\in\mathcal{J}} \beta^t_{i,j,c} \leq 1, \quad \forall c \in \mathcal{C}$$
$$\text{D5}: \sum_{i\in\mathcal{I}}\sum_{j\in\mathcal{J}} \gamma^t_{i,j,q} \leq 1, \quad \forall q \in \mathcal{Q}_k$$
$$\text{D6}: \sum_{k\in\mathcal{K}}\sum_{c\in\mathcal{C}} \alpha^t_{i,j,k}\beta^t_{i,j,c} \geq X^{t*}_{i,j},$$

$$\begin{aligned} & \forall i \in \mathcal{I},\ j \in \mathcal{J}_{\mathrm{UR}} \\ \mathrm{D7}: & \sum_{q \in \mathcal{Q}_k} \alpha^t_{i,j,k} \gamma^t_{i,j,q} \geq Y^{t*}_{i,j}, \\ & \forall i \in \mathcal{I},\ j \in \mathcal{J}_{\mathrm{UR}},\ k \in \mathcal{K} \\ \text{variables}: \quad & \beta^t_{i,j,c} \in \{0,1\}, \quad \forall i \in \mathcal{I},\ j \in \mathcal{J},\ c \in \mathcal{C} \\ & \gamma^t_{i,j,q} \in \{0,1\}, \quad \forall i \in \mathcal{I},\ j \in \mathcal{J},\ q \in \mathcal{Q}_k \end{aligned} \tag{2}$$

where $\alpha^t_{i,j,k}$ is the association variable such that $\alpha^t_{i,j,k} = 1$ when vehicle i's application task j is associated with RSU k for task offloading at each time slot t, and $\alpha^t_{i,j,k} = 0$ otherwise. For the sake of simplicity, we consider that $\alpha^t_{i,j,k}$ is predetermined by $\alpha^t_{i,j,k} = 1$ if vehicle i has the most close distance to RSU k. The first decision variable $\beta^t_{i,j,c}$ is the channel allocation variable such that $\beta^t_{i,j,c} = 1$ when vehicle i's application task j is selected to transmit on channel c at each time slot t, and $\beta^t_{i,j,c} = 0$ otherwise. The second decision variable $\gamma^t_{i,j,q}$ is the computation resource allocation variable such that $\gamma^t_{i,j,q} = 1$ when vehicle i's application task j is selected to utilize computation resource q at each time slot t, and $\gamma^t_{i,j,q} = 0$ otherwise. The objective of $\mathcal{P}2$ aims to minimize the overall task offloading delay, where the delay $d^t_{i,j}$ for offloading each vehicle i's application task j at time slot t can be calculated as follows:

$$d^t_{i,j} = \frac{S^t_{i,j}}{\sum_{k \in \mathcal{K}} \sum_{c \in \mathcal{C}} \alpha^t_{i,j,k} \beta^t_{i,j,c} R^t_{i,j,k,c}} + \frac{S^t_{i,j}}{\sum_{k \in \mathcal{K}} \sum_{q \in \mathcal{Q}_k} \alpha^t_{i,j,k} \gamma^t_{i,j,q} W^t_{k,q}} \tag{3}$$

The first part of Eq. (3) represents the communication delay, where $S^t_{i,j}$ is the application task size. And $R^t_{i,j,k,c}$ is the communication rate, which is calculated as follows:

$$R^t_{i,j,k,c} = B \log_2 \left(1 + \frac{p^t_{i,j,k,c} g^t_{i,j,k,c}}{N_0 + I_{\mathrm{cell}}}\right) \tag{4}$$

where $p^t_{i,j,k,c}$ is the uplink transmit power of vehicle i's application j to RSU k on channel c at time slot t, $g^t_{i,j,k,c}$ is the channel gain of vehicle i's application j to RSU k on channel c at time slot t. B is the channel bandwidth, N_0 is the white Gaussian noise power, and I_{cell} is the co-channel interference of cellular users to vehicular users. In this paper, we assume that $p^t_{i,j,k,c}$ and I_{cell} are all given, and thus, the value of $R^t_{i,j,k,c}$ can be determined under given channel allocation results. The second part of Eq. (3) represents the computation delay, where $W^t_{k,q}$ is the computation rate of computation resource k of RSU q at time slot t.

In problem $\mathcal{P}2$, constraint D1 guarantees that the maximum number of associated channels for task offloading cannot exceed $|\mathcal{C}|$. Constraint D2 guarantees that the maximum number of associated computation resources for task offloading on each RSU cannot exceed $|\mathcal{Q}_k|$. Constraint D3 guarantees that each vehicle's application can be associated with at most one RSU. Constraints D4 and D5 guarantee that each vehicle's application can be allocated with at most one channel and computation resource, respectively. Constraints D6 and D7 ensure that, for URLLC application tasks, the total number of allocated channel and computation resources should be no less than the reserved value. Problem $\mathcal{P}2$ is a typical binary nonlinear programming problem, and there is no general algorithm that can achieve the globally optimal solution. Moreover, Problem $\mathcal{P}2$ is NP-hard.

1) Problem Connection Analysis: The connection between problem $\mathcal{P}1$ and problem $\mathcal{P}2$ is that problem $\mathcal{P}2$ is based on the optimized solutions of problem $\mathcal{P}1$. Details are analyzed as follows. Constraints D6 and D7 in $\mathcal{P}2$ utilize the optimized solutions of $\mathcal{P}1$, i.e., $X^{t*}_{i,j}$ and $Y^{t*}_{i,j}$, as the resource allocation constraints. Specifically, Constraint D6 means that the allocated channel number of vehicle i's URLLC task j should be no smaller than the optimized reservation number $X^{t*}_{i,j}$. And Constraint D7 means that the allocated computation resource number of vehicle i's URLLC task j should be no smaller than the optimized reservation number $Y^{t*}_{i,j}$.

V. Solving the Resource Reservation Problem

The goal of problem $\mathcal{P}1$ is to maximize the resource utilization while satisfying the necessary resource demand constraints. The obtained solution is input into the physical domain as a part problem $\mathcal{P}2$'s constraints. The objective of problem $\mathcal{P}2$ is to minimize the overall task offloading delay based on the optimized solution from problem $\mathcal{P}1$. Therefore, in the section, we first introduce the solution to problem $\mathcal{P}1$.

We first introduce a robust optimization method to solve the resource reservation problem, i.e., problem $\mathcal{P}1$. The robust optimization presents a robust parameter based approach for handling the tradeoff between the problem uncertainty and solution optimality degree [36], [37]. In our study, the problem uncertainty is represented by the number of DT's inaccurate predictions (corresponding to $\widehat{C}^t_{i,j} \neq 0$ or $\widehat{Q}^t_{i,j} \neq 0$ in constraints C3 or C4 of problem $\mathcal{P}1$) which can be handled by the robust parameter. For realization, we first reformulate problem $\mathcal{P}1$ by decoupling it into two parallel sub-problems. Then, we introduce the robust parameter Γ_i to control the maximum number of uncertain coefficients in the ith sub-constraint of either C3 or C4. After Γ_i is given, we can obtain the feasible solution of problem $\mathcal{P}1$ by transforming it into an integer programming problem, which can be solved by standard integer optimization tools. In addition, we show that the proposed robust solution is feasible (i.e., the transformation loss is tolerable) by proving that the constraint violation probability regarding the robust parameter is upper bounded by a maximum value.

A. Finding the Feasible Solution Under Given Γ_i

The original problem $\mathcal{P}1$ in Eq. (1) can be equivalently transformed into the following problem at each individual time slot t:

$$\begin{aligned} \min \quad & \sum_{i \in \mathcal{I}} \sum_{j \in \mathcal{J}_{\mathrm{UR}}} \epsilon_1 X^t_{i,j} + \epsilon_2 Y^t_{i,j} \\ \text{s.t.} \quad & \mathrm{C1} - \mathrm{C2} \\ & \mathrm{C3}': \sum_{j \in \mathcal{J}_{\mathrm{UR}}} \tilde{A}^t_{i,j} X^t_{i,j} \geq \Psi^1_i, \quad \forall i \in \mathcal{I} \\ & \mathrm{C4}': \sum_{j \in \mathcal{J}_{\mathrm{UR}}} \tilde{B}^t_{i,j} Y^t_{i,j} \geq \Psi^2_i, \quad \forall i \in \mathcal{I} \end{aligned}$$

$$\begin{aligned} &\text{variables}: X^t_{i,j} \in \mathbb{N}, \quad \forall i \in \mathcal{I}, j \in \mathcal{J}_{\text{UR}} \\ &\qquad\quad Y^t_{i,j} \in \mathbb{N}, \quad \forall i \in \mathcal{I}, j \in \mathcal{J}_{\text{UR}} \end{aligned} \tag{5}$$

where $\tilde{A}^t_{i,j}$ and $\tilde{B}^t_{i,j}$ are the equivalent uncertain constraint parameters in the values of $\left[A^t_{i,j}-\widehat{A}^t_{i,j}, A^t_{i,j}+\widehat{A}^t_{i,j}\right]$ and $\left[B^t_{i,j}-\widehat{B}^t_{i,j}, B^t_{i,j}+\widehat{B}^t_{i,j}\right]$, respectively. Specifically, we have:

$$\tilde{A}^t_{i,j} = \frac{1}{2}\left(\frac{1}{(C^t_{i,j}-\widehat{C}^t_{i,j})}+\frac{1}{(C^t_{i,j}+\widehat{C}^t_{i,j})}\right) \tag{6a}$$

$$\widehat{A}^t_{i,j} = \frac{1}{2}\left(\frac{1}{(C^t_{i,j}-\widehat{C}^t_{i,j})}-\frac{1}{(C^t_{i,j}+\widehat{C}^t_{i,j})}\right) \tag{6b}$$

$$\tilde{B}^t_{i,j} = \frac{1}{2}\left(\frac{1}{(Q^t_{i,j}-\widehat{Q}^t_{i,j})}+\frac{1}{(Q^t_{i,j}+\widehat{Q}^t_{i,j})}\right) \tag{6c}$$

$$\widehat{B}^t_{i,j} = \frac{1}{2}\left(\frac{1}{(Q^t_{i,j}-\widehat{Q}^t_{i,j})}-\frac{1}{(Q^t_{i,j}+\widehat{Q}^t_{i,j})}\right) \tag{6d}$$

where the equivalence between eq. (1) and eq. (5) is proved in Appendix I. The optimization problem in eq. (5) has the following features. First, $\epsilon_1 X^t_{i,j}$ and $\epsilon_2 Y^t_{i,j}$ are independent and separable parts of the sum objective. Second, constraints C1 and C3' are only associated with $X^t_{i,j}$, and C2 and C4' are only associated with $Y^t_{i,j}$. Therefore, we can divide problem (5) into the following two independent sub-problems (7) and (8):

$$\begin{aligned} &\min \quad \sum_{i\in\mathcal{I}}\sum_{j\in\mathcal{J}_{\text{UR}}} \epsilon_1 X^t_{i,j} \\ &\text{s.t.} \quad \text{C1, C3}': \sum_{j\in\mathcal{J}_{\text{UR}}} \tilde{A}^t_{i,j} X^t_{i,j} \geq \Psi^1_i, \quad \forall i \in \mathcal{I} \\ &\text{variables}: X^t_{i,j} \in \mathbb{N}, \forall i \in \mathcal{I}, j \in \mathcal{J}_{\text{UR}} \end{aligned} \tag{7}$$

$$\begin{aligned} &\min \quad \sum_{i\in\mathcal{I}}\sum_{j\in\mathcal{J}_{\text{UR}}} \epsilon_2 Y^t_{i,j} \\ &\text{s.t.} \quad \text{C2, C4}': \sum_{j\in\mathcal{J}_{\text{UR}}} \tilde{B}^t_{i,j} Y^t_{i,j} \geq \Psi^2_i, \quad \forall i \in \mathcal{I} \\ &\text{variables}: Y^t_{i,j} \in \mathbb{N}, \forall i \in \mathcal{I}, j \in \mathcal{J}_{\text{UR}} \end{aligned} \tag{8}$$

where sub-problem (7) corresponds to find the optimal $X^t_{i,j}$, and sub-problem (8) corresponds to find the optimal $Y^t_{i,j}$. Let us first turn to solve sub-problem (7). As analyzed before, the URLLC task requirements predicted by DT can be partly inaccurate. Thus, we introduce a robust parameter Γ_i to represent the inaccuracy degree of the DT prediction, or constraint uncertainty degree in the optimization problem. Γ_i is defined as follows [37]: For every i, Γ_i takes values in the interval $\left[0, |\mathcal{J}_{i,\text{UR}}|\right]$, which is not necessarily integer. $\mathcal{J}_{i,\text{UR}}$ represents vehicle i's URLLC task set. The parameter Γ_i is to adjust the tradeoff between the problem uncertainty degree against the solution optimality. The problem uncertainty degree represents how many uncertain constraints can be handled out of the overall uncertainty coefficients in C3' (or C4'). The robust parameter aims to handle the case that, for given i and Γ_i, up to $\lfloor\Gamma_i\rfloor$ of the coefficients $\tilde{A}^t_{i,j}$, $j \in \mathcal{J}_{i,\text{UR}}$ are allowed to change by $\widehat{A}^t_{i,j}$, and meanwhile there exists another one coefficient changing by $(\Gamma_i - \lfloor\Gamma_i\rfloor)\widehat{A}^t_{i,j}$.

1) Handling the Uncertain Constraints: Based on the above definition of Γ_i, we can first introduce $\mathcal{U}_i$ as the task set of vehicle i with uncertain communication demand $\widehat{C}^t_{i,j} \neq 0$, $\tilde{A}^t_{i,j} \neq 0$, which can be handled by Γ_i. Obviously, we have $\mathcal{U}_i \subset \mathcal{J}_{i,\text{UR}}$ and $|\mathcal{U}_i| = \lfloor\Gamma_i\rfloor + 1$. Afterwards, we construct eq. (9), shown at the bottom of the next page, for handling the uncertain coefficients of constraint C3' in eq. (7). Eq. (9) is written by separating the deterministic and uncertain parts of $\tilde{A}^t_{i,j}$ of constraint C3' in eq. (7). The first part of eq. (9) is the deterministic coefficient, and the second part is the uncertain coefficient. In eq. (9), l_i is used as the temporary index of the application task. And $\mathcal{S}_i$ is the subset with uncertain coefficients where $\mathcal{S}_i \subseteq \mathcal{U}_i, |\mathcal{S}_i| = \lfloor\Gamma_i\rfloor$. For convenience, we use $\rho_i\left(\{X^t_{i,j}\}, \Gamma_i\right)_{j\in\mathcal{U}_i}$, which is defined in eq.(10), to represent the second part of eq. (9). Thus, we can define that the ith sub-constraint of C3' is protected by $\rho_i\left(\{X^t_{i,j}\}, \Gamma_i\right)_{j\in\mathcal{U}_i}$ according to eq. (9), where $\rho_i\left(\{X^t_{i,j}\}, \Gamma_i\right), j \in \mathcal{U}_i$ can be referred as the protection function. The meaning of "protection" is two-fold. First, $\rho_i\left(\{X^t_{i,j}\}, \Gamma_i\right)_{j\in\mathcal{U}_i}$ takes the maximization operator, which is the worst case for satisfying the inequality (9). Second, subtraction and addition should be both considered between the deterministic and uncertain coefficients. Since $\rho_i\left(\{X^t_{i,j}\}, \Gamma_i\right)_{j\in\mathcal{U}_i} \geq 0$, subtraction can be adopted instead of addition, making it the worst case for satisfying the inequality (9). Based on the definition of protection function, we can introduce the following proposition.

Proposition 1: Given Γ_i, $X^t_{i,j}$, i and t, the protection function of the ith sub-constraint of C3', which can be written as:

$$\begin{aligned} &\rho_i\left(\{X^t_{i,j}\}, \Gamma_i\right) \\ &= \max_{\left\{\mathcal{S}_i\cup\{l_i\} | \mathcal{S}_i\subseteq\mathcal{U}_i, |\mathcal{S}_i|=\lfloor\Gamma_i\rfloor, l_i\in\mathcal{U}_i\setminus\mathcal{S}_i\right\}} \\ &\left\{\sum_{j\in\mathcal{S}_i} \widehat{A}^t_{i,j} X^t_{i,j} + (\Gamma_i - \lfloor\Gamma_i\rfloor)\widehat{A}_{i,l_i} X^t_{i,l_i}\right\} \end{aligned} \tag{10}$$

which equals to the objective function in the following linear optimization:

$$\begin{aligned} \rho_i\left(\{X^t_{i,j}\}, \Gamma_i\right) = \ &\max \sum_{j\in\mathcal{U}_i} \hat{A}^t_{i,j} X^t_{i,j} Z^t_{i,j} \\ &\text{s.t.} \sum_{j\in\mathcal{U}_i} Z^t_{i,j} \leq \Gamma_i \\ &0 \leq Z^t_{i,j} \leq 1, \ \forall j \in \mathcal{U}_i \\ &\text{variables}: Z^t_{i,j}, \quad \forall j \in \mathcal{U}_i \end{aligned} \tag{11}$$

Proof: The optimal solution value of problem (11) consists of $|\mathcal{U}_i| - 1 = \lfloor\Gamma_i\rfloor$ variables at 1 and one variable at $\Gamma_i - (|\mathcal{U}_i| - 1) = \Gamma_i - \lfloor\Gamma_i\rfloor$. This is equivalent to the selection of subset $\left\{\mathcal{S}_i \cup \{l_i\} | \mathcal{S}_i \subseteq \mathcal{U}_i, |\mathcal{S}_i| = \lfloor\Gamma_i\rfloor, l_i \in \mathcal{U}_i \setminus \mathcal{S}_i\right\}$ with the corresponding function $\sum_{j\in\mathcal{S}_i} \widehat{A}^t_{i,j} X^t_{i,j} + (\Gamma_i - \lfloor\Gamma_i\rfloor)\widehat{A}_{i,l_i} X^t_{i,l_i}$ of the protection function $\rho_i\left(\{X^t_{i,j}\}, \Gamma_i\right), j \in \mathcal{U}_i$. Note that $Z^t_{i,j}$ is the temporary variable for the convenience of problem transformation. This completes the proof of *Proposition 1*.

Based on the above proposition, we can transform sub-problem (7) into the integer programming problem as follows.

Proposition 2: Sub-problem (7) can be transformed into the following integer programming formulation:

$$\begin{aligned}
&\min \sum_{i\in\mathcal{I}}\sum_{j\in\mathcal{J}_{\mathrm{UR}}} \epsilon_1 X_{i,j}^t \\
&\text{s.t.} \quad \sum_{i\in\mathcal{I}}\sum_{j\in\mathcal{J}_{\mathrm{UR}}} X_{i,j}^t \le |\mathcal{C}| \\
&\quad \sum_{j\in\mathcal{J}_{\mathrm{UR}}} A_{i,j}^t X_{i,j}^t - \sum_{j\in\mathcal{U}_i} U_{i,j}^t - \Gamma_i Z_i^t \ge \Psi_i^1, \quad \forall i\in\mathcal{I} \\
&\quad Z_i^t + U_{i,j}^t \ge \hat{A}_{i,j}^t X_{i,j}^t, \quad \forall i\in\mathcal{I}, j\in\mathcal{U}_i \\
&\text{variables}: X_{i,j}^t \in \mathbb{N}, \ \forall i\in\mathcal{I}, j\in\mathcal{J}_{\mathrm{UR}} \\
&\quad U_{i,j}^t \ge 0, \quad \forall i\in\mathcal{I}, j\in\mathcal{U}_i \\
&\quad Z_i^t \ge 0, \quad \forall i\in\mathcal{I}
\end{aligned} \tag{12}$$

Proof: First, we derive the duality of problem (11):

$$\begin{aligned}
&\min \sum_{j\in\mathcal{U}_i} U_{i,j}^t + \Gamma_i Z_i^t \\
&\text{s.t.} \quad Z_i^t + U_{i,j}^t \ge \hat{A}_{i,j}^t X_{i,j}^t, \ \forall j\in\mathcal{U}_i \\
&\text{variables}: U_{i,j}^t \ge 0, \ \forall j\in\mathcal{U}_i \\
&\quad Z_i^t \ge 0
\end{aligned} \tag{13}$$

where we can observe that problems (11) and (13) are feasible and their objective values achieve strong duality. Note that this can be achieved through standard convex optimization theory by swapping the logic of objectives and constraints between problem (11) and (13). Based on *Proposition 1*, we know that $\rho_i\left(\{X_{i,j}^t\},\Gamma_i\right)_{j\in\mathcal{U}_i}$ is equal to the objective function of problem (13). Therefore, we can substitute (13) to (9), which helps eliminate and transform the uncertain coefficients of constraint C3' in problem (7) into the constraints in (12) with deterministic coefficients (i.e., the 2nd and 3rd constraints). Note that the first constraint of (12) is the constraint C1 of problem (7). This completes the proof of *Proposition 2*.

To this end, we have transformed the original problem (7) into the equivalent problem (12), which can be solved by standard integer optimization tools [38] under the given robust parameter Γ_i. Since problem (7) and problem (8) are two parallel sub-problems, problem (8) can be also solved in the same way as problem (7) by introducing a new parameter Γ_i and deriving its equivalent problem. By conclusion, our proposed method aims to transform the constraint C3' with uncertain coefficients into the equivalent constraint set of certain coefficients. In the next part, we will analyze the feasibility of our proposed solutions.

B. Solution Feasibility Analysis

1) Problem Transformation Loss Analysis: It should be noted that the definition of Γ_i for handling the uncertain constraints is that, for given i and Γ_i, up to $\lfloor\Gamma_i\rfloor$ of the coefficients $\tilde{A}_{i,j}^t$, $j\in\mathcal{J}_{i,\mathrm{UR}}$ are allowed to change by $\widehat{A}_{i,j}^t$, and meanwhile there exists another one coefficient changing by $(\Gamma_i-\lfloor\Gamma_i\rfloor)\widehat{A}_{i,j}^t$. This is not equivalent to the original constraint C3' where for given i, the uncertain coefficient $\tilde{A}_{i,j}^t$, $j\in\mathcal{J}_{i,\mathrm{UR}}$ of the uncertain constraints changes by $\widehat{A}_{i,j}^t$, $j\in\mathcal{J}_{i,\mathrm{UR}}$. Note that Γ_i takes values in the interval $\left[0,|\mathcal{J}_{i,\mathrm{UR}}|\right)$. This can cause the problem transformation loss. Therefore, in this part, we show that the proposed solutions are feasible, i.e. the problem transformation loss is tolerable, by proving that the transformation loss, or violation of C3' is limited to a maximum probability. Specifically, we introduce the following proposition [37].

Proposition 3: Given a specific ith sub-constraint of C3', let $\{x_j^*\}$, $j\in\mathcal{J}_{\mathrm{UR}}$ be an optimal solution set of problem (12). Let $\mathcal{S}_i^*$ and l_i^* be the set and the index which achieve the minimum value of $\rho_i\left(\{X_{i,j}^t\},\Gamma_i\right)_{j\in\mathcal{U}_i}$. Let us define the uncertain variable $\eta_{i,j}=(\tilde{A}_{i,j}^t-A_{i,j}^t)/\widehat{A}_{i,j}^t$, $j\in\mathcal{U}_i$, which obeys an unknown, but symmetric distribution, and takes values in [-1,1].

(a) The probability that the ith sub-constraint of C3' is violated satisfies:

$$\mathrm{P_r}\left(\sum_{j\in\mathcal{J}_{\mathrm{UR}}}\tilde{A}_{i,j}^t x_j^* < \Psi_i^1\right) \le \mathrm{P_r}\left(\sum_{j\in\mathcal{U}_i}\gamma_{i,j}\eta_{i,j}\le\Gamma_i\right) \tag{14}$$

where

$$\gamma_{ij}=\begin{cases}1, & \text{if } j\in\mathcal{S}_i^* \\ \frac{\hat{A}_{i,j}^t x_j^*}{\hat{A}_{i,r^*}^t x_{r^*}^*}, & \text{if } j\in\mathcal{U}_i\backslash\mathcal{S}_i^*\end{cases} \tag{15}$$

and

$$r^*=\arg\max_{r\in\mathcal{S}_i^*\cup\{l_i^*\}}\hat{A}_{i,r}x_r^* \tag{16}$$

(b) The values of $\gamma_{i,j}$ satisfy $\gamma_{i,j}\le 1$, $\forall\ j\in\mathcal{U}_i\backslash\mathcal{S}_i^*$.

The proof of *Proposition 3* is given in Appendix II. Eq. (14) means that, by using the proposed robust parameter based solutions, the violation probability of C3' (the left part) is upper bounded by the maximum probability (the right part) of (14). And we can observe that as Γ_i increases, the upper bounded probability for the uncertain constraint violation is also increased. The reason is that the problem transformation loss is increased as the number for handling the uncertain problem constraints increases.

VI. Solving the Task Offloading Problem

To reduce the complexity of the task offloading problem $\mathcal{P}2$ in Eq. (2), we decouple $\mathcal{P}2$ by considering each decision variable $\beta_{i,j,c}^t$ and $\gamma_{i,j,q}^t$, respectively. The rationality of the problem decoupling is based on the fact that $S_{i,j}^t$ is a pre-determined parameter in Eq. (3). Thus, the communication delay and computation delay can be determined by the independent channel allocation variable $\alpha_{i,j,k}^t$ and computation

$$\sum_{j\in\mathcal{J}_{\mathrm{UR}}}A_{i,j}^t X_{i,j}^t - \max_{\left\{\mathcal{S}_i\cup\{l_i\}\,|\,\mathcal{S}_i\subseteq\mathcal{U}_i,|\mathcal{S}_i|=\lfloor\Gamma_i\rfloor,l_i\in\mathcal{U}_i\backslash\mathcal{S}_i\right\}}\left\{\sum_{j\in\mathcal{S}_i}\widehat{A}_{i,j}^t X_{i,j}^t+(\Gamma_i-\lfloor\Gamma_i\rfloor)\widehat{A}_{i,l_i}X_{i,l_i}^t\right\}\ge\Psi_i^1, \quad \forall i\in\mathcal{I} \tag{9}$$

resource allocation variable $\beta^t_{i,j,k}$, respectively. In the future, we will jointly consider the optimization of task segmentation, channel resource allocation and computation resource allocation decisions.

First, we solve the channel allocation sub-problem. Second, we solve the computation resource allocation sub-problem. We decouple the sub-problem $\mathcal{S}1$ from the original problem $\mathcal{P}2$ as follows:

$$\begin{aligned} \mathcal{S}1: \quad & \min \sum_{i\in\mathcal{I}}\sum_{j\in\mathcal{J}} d^t_{i,j} \\ & \text{s.t.} \quad \text{D1, D4, D6} \\ & \text{variables}: \beta^t_{i,j,c} \in \{0,1\}, \forall i \in \mathcal{I}, j \in \mathcal{J}, c \in \mathcal{C} \end{aligned} \tag{17}$$

Considering that the sub-problem $\mathcal{S}1$ presents a mutual association between vehicular tasks and channel resources, we introduce matching theory to solve it. Matching theory has been proved efficient due to its ability in defining association preference relations between the matching individuals and reducing complexity for large-scale resource allocation problems [39], [40]. Therefore, in the following part, we will first present the matching framework for the sub-problem $\mathcal{S}1$, and then define the preference functions for the users and the channels. Based on constraints D1 and D4, we can re-formulate the sub-problem $\mathcal{S}1$ as a many-to-one matching.

Definition 1: A many-to-one matching Θ is defined as a mapping: $\mathcal{C}\cup(\mathcal{I},\mathcal{J}) \to \mathcal{C}\cup(\mathcal{I},\mathcal{J})$, such that (1) $|\Theta(c)| \le 1$; (2) $|\Theta(i,j)| \le \mathcal{C}$; (3) $\Theta(c) = \{i \in \mathcal{I}, j \in \mathcal{J} | c \to (i,j) \in \Theta\}$ and $\Theta(i,j) = \{i \in \mathcal{I}, j \in \mathcal{J} | (i,j) \to c \in \Theta\}$.

A. Vehicular Task Preference

Based on Eq. (3), we know that the objective of task processing delay in (17) is prominently determined by the V2X communication data rate. The preference of vehicle i's task j over channel c is defined as the V2X achieved data rate of user i's task j allocated with channel c:

$$F^t_{i,j}(c) = R^t_{i,j,k,c} \tag{18}$$

B. Channel Preference

The preference of channel c over vehicle i's task j is defined as the priority level of vehicle i in the current time t:

$$F^t_c(i,j) = E^t_{i,j,c} \tag{19}$$

where the priority level is introduced to guarantee the channel allocation fairness, which can be defined as follows:

$$E^t_{i,j,c} = \frac{1}{T^t_{i,j,c}+1}, 0 \le T^t_{i,j,c} \le \Delta t \tag{20}$$

where $T^t_{i,j,c}$ records the number of time slots in which vehicle i's task j is allocated with channels during time slot interval $[t-\Delta t, t]$. Thus, channel c has the incentive to reject the user task of low priority. The priority level of the rejected user task will be improved in future time slots to achieve higher channel allocation probability.

The matching algorithm for associating the URLLC and non-URLLC tasks with the channel resources is presented in **Algorithm 1**, which includes two parts. The first part is a two-sided many-to-one matching for the URLLC tasks (lines 2-11). The URLLC tasks first send matching requests to their most preferred channels based on the preference functions as defined in Eq. (18) (lines 3-6). The channels wait to collect the matching requests and then choose the most preferred users based on the preference functions defined in Eq. (19), and reject other tasks (lines 7-11) on the condition that the allocated channel number doesn't exceed the reserved channel number. After the URLLC channel allocation is finished, the non-URLLC tasks send matching requests to their most preferred channels based on their preference functions as defined in eq. (18) (lines 13-16). The channels wait to collect the matching requests and then choose the most preferred users based on the preference functions defined in Eq. (19), and reject other users (lines 17-20).

C. Complexity

In line 2-11 of **Algorithm 1**, the worst-case scenario occurs when all URLLC user traffics ($i \in \mathcal{I}$, $j \in \mathcal{J}_{\text{UR}}$) have the same preferences on all channels (i.e., all URLLC user traffics have the same preference list). In this case, all URLLC user traffics ask for the same channel with the best preference value, while other channels receive empty matching requests at each iteration. Thus, it requires $|\mathcal{I}|\times|\mathcal{J}_{\text{UR}}|\times|\mathcal{C}|$ number of iterations to finish the matching process. In similar, line 12-20 of **Algorithm 1** requires $|\mathcal{I}|\times|\mathcal{J}-\mathcal{J}_{\text{UR}}|\times|\mathcal{C}|$ number of iterations to finish the matching process. In overall, the complexity of **Algorithm 1** is $\mathcal{O}\big(|\mathcal{I}|\times|\mathcal{J}_{\text{UR}}|\times|\mathcal{C}|+|\mathcal{I}|\times|\mathcal{J}-\mathcal{J}_{\text{UR}}|\times|\mathcal{C}|\big)$.

Next, we decouple the sub-problem $\mathcal{S}2$ from the original problem $\mathcal{P}2$ by considering the computation resource allocation variable $\gamma^t_{i,j,q}$:

$$\begin{aligned} \mathcal{S}2: \quad & \min \sum_{\text{i}\in\mathcal{I}}\sum_{\text{j}\in\mathcal{J}} \text{d}^{\text{t}}_{\text{i,j}} \\ & \text{s.t.} \quad \text{D2, D5, D7} \\ & \text{variables}: \gamma^t_{i,j,q} \in \{0,1\}, \forall i \in \mathcal{I}, j \in \mathcal{J}, q \in \mathcal{Q}_k \end{aligned} \tag{21}$$

where from constraints D2 and D5, we observe that the sub-problem $\mathcal{S}2$ can be also considered as a many-to-one matching between the computation resources and the user task (similar to **Definition 1**). Therefore, we define the preference functions of the vehicular task and computation resources as follows.

D. Vehicular Task Preference

Based on Eq. (3), we know that the objective of task processing delay in (21) is prominently determined by the computation speed of the computation resources. Thus, the preference of vehicle i's task j over computation resource q is defined as q's computation speed:

$$F^t_{i,j}(q) = W^t_{k,q} \tag{22}$$

E. Computation Resource Preference

The preference of computation resource q over vehicle i's task j is defined as the priority level of vehicle i in the current time t:

$$F^t_q(i,j) = E^t_{i,j,q} \tag{23}$$

Algorithm 1 Channel Resource Matching

1 *Initialize*: $\beta^t_{i,j,c} = 0, \forall i, j, c$;
2 **while** *the matching is not stable* **do**
3 **for** $i \in \mathcal{I}$ **do**
4 **for** $j \in \mathcal{J}_{UR}$ **do**
5 $\widehat{c} = \arg\max_{c \in \mathcal{C}} F^t_{i,j}(c)$;
6 User i's task j sends matching requests to channel $\widehat{c}$;
7 **for** $c \in \mathcal{C}$ **do**
8 c waits to collect all the requests;
9 **if** $\sum_{c \in \mathcal{C}} \beta^t_{i,j,c} < X^{t*}_{i,j}$ **then**
10 $(\hat{i}, \hat{j}) = \arg\max_{(i,j) \in \chi} \left(F^t_c(i, j)\right)$;
11 Set $\beta^t_{\hat{i},\hat{j},c} = 1$, delete c from $\mathcal{C}$;
12 **while** *the matching is not stable* **do**
13 **for** $i \in \mathcal{I}$ **do**
14 **for** $j \in \mathcal{J} - \mathcal{J}_{UR}$ **do**
15 $\widehat{c} = \arg\max_{c \in \mathcal{C}} F^t_{i,j}(c)$;
16 User i's task j sends matching requests to channel $\widehat{c}$;
17 **for** $c \in \mathcal{C}$ **do**
18 c waits to collect all the requests;
19 $(\hat{i}, \hat{j}) = \arg\max_{(i,j) \in \chi} \left(F^t_c(i, j)\right)$;
20 Set $\beta^t_{\hat{i},\hat{j},c} = 1$, delete c from $\mathcal{C}$;

where the priority level is introduced to guarantee the computation resource allocation fairness, which can be defined as follows:

$$E^t_{i,j,q} = \frac{1}{T^t_{i,j,q} + 1}, 0 \le T^t_{i,j,q} \le \Delta t \tag{24}$$

where $T^t_{i,j,q}$ records the number of time slots in which vehicle i's task j is allocated with computation resources during time interval $[t - \Delta t, t]$. Larger $T^t_{i,j,q}$ means that vehicle i's task j has been allocated with more resources in time interval $[t - \Delta t, t]$, and thus the resource allocation priority is lowered to guarantee fairness. By contrast, the priority level of the rejected vechicular task will be improved in future time slots to achieve higher computation resource allocation probability.

The matching algorithm for allocating the URLLC and the non-URLLC tasks with the computation resources is presented in **Algorithm 2**, which includes two parts. The first part is a two-sided many-to-one matching for the URLLC tasks (lines 1-11). The URLLC tasks first send matching requests to their most preferred computation resources based on the preference functions as defined in Eq. (22) (lines 3-6). The computation resources wait to collect the matching requests and then choose the most preferred tasks based on the preference functions defined in Eq. (23), and reject other tasks (lines 7-11) on the condition that the allocated computation resource number doesn't exceed the reserved number.

After all the URLLC computation resource allocation is finished, the non-URLLC tasks send matching requests to their most preferred computation resources based on their preference functions as defined in Eq. (22) (lines 13-16). The computation resources wait to collect the matching requests and then choose the most preferred tasks based on the preference functions defined in Eq. (23), and reject other tasks (lines 17-20). Similarly, the complexity of **Algorithm 2** is $\mathcal{O}\big(|\mathcal{I}| \times |\mathcal{J}_{\mathrm{UR}}| \times |\mathcal{Q}_k| + |\mathcal{I}| \times |\mathcal{J} - \mathcal{J}_{\mathrm{UR}}| \times |\mathcal{Q}_k|\big)$.

Algorithm 2 Computation Resource Matching

1 *Initialize*: $\gamma^t_{i,j,q} = 0, \forall i, j, q$;
2 **while** *the matching is not stable* **do**
3 **for** $i \in \mathcal{I}$ **do**
4 **for** $j \in \mathcal{J}_{UR}$ **do**
5 $\widehat{q} = \arg\max_{q \in \mathcal{Q}_k} F^t_{i,j}(q)$;
6 User i's task j sends matching requests to computation resource $\widehat{q}$;
7 **for** $q \in \mathcal{Q}_k$ **do**
8 q waits to collect all the requests;
9 **if** $\sum_{q \in \mathcal{Q}_k} \gamma^t_{i,j,q} < Y^{t*}_{i,j}$ **then**
10 $(\hat{i}, \hat{j}) = \arg\max_{(i,j) \in \chi} \left(F^t_q(i, j)\right)$;
11 Set $\gamma^t_{\hat{i},\hat{j},q} = 1$, delete q from $\mathcal{Q}_k$;
12 **while** *the matching is not stable* **do**
13 **for** $i \in \mathcal{I}$ **do**
14 **for** $j \in \mathcal{J} - \mathcal{J}_{UR}$ **do**
15 $\widehat{q} = \arg\max_{q \in \mathcal{Q}_k} F^t_{i,j}(q)$;
16 User i's task j sends matching requests to computation resource $\widehat{q}$;
17 **for** $q \in \mathcal{Q}_k$ **do**
18 q waits to collect all the requests;
19 $(\hat{i}, \hat{j}) = \arg\max_{(i,j) \in \chi} \left(F^t_q(i, j)\right)$;
20 Set $\gamma^t_{\hat{i},\hat{j},q} = 1$, delete q from $\mathcal{Q}_k$;

VII. Simulation and Analysis

In this section, we first construct the DT simulator of our proposed model by importing realistic roadmap into SUMO. SUMO can perform vehicular safety prediction and thus help to predict the URLLC task requirement. Based on the prediction results, we evaluate the performance of our proposed robust optimization based resource reservation. Then, we compare the performance of our proposed resource reservation and task offloading scheme with two benchmarks.

A. DT Construction and Vehicular Safety Prediction

As shown in Fig. 2 (left part), we select G2 Beijing-Shanghai Highway as the realistic roadmap. The selected area is a bi-directional four-lane road sector (i.e., two lanes in each direction), with each lane of 3.6 meters in width. We select the 1 kilometers (km) length sector as the simulated area, as shown

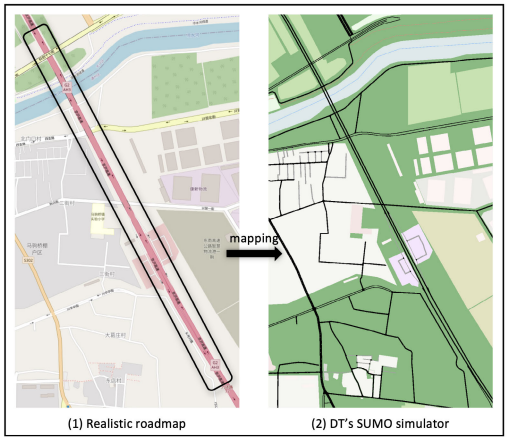

Fig. 2. The mapping of realistic roadmap to DT's SUMO simulator.

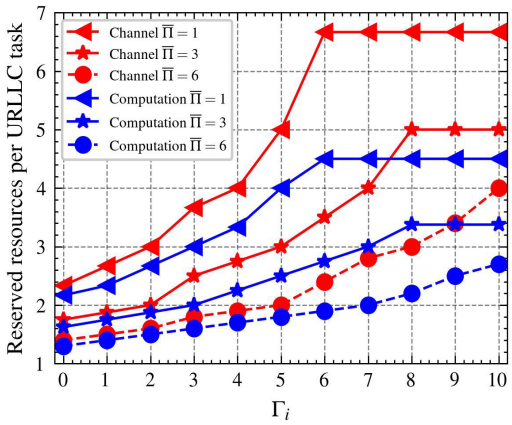

Fig. 3. Reserved resources per URLLC task versus Γ_i.

in Fig. 2. The realistic road structure, speed limitation and vehicle density are mapped into the SUMO simulator, as in Fig. 2. The maximum speed limitation is 90 km/h. The vehicle density takes 20 per lane per km, which is estimated based on the road traffic condition collected during 11:00-11:15 on 15th, May, 2023. In the SUMO simulator, the Intelligent Driver Model (IDM) [41] is used for simulating the vehicle-following behaviours. The IDM is a classic vehicle-following model, which considers a driver's desire to maintain a safe distance from the front vehicle while also achieving the desired speed. The safety control utilizes a lane-changing model based on a reinforcement learning strategy of our previous study [35], where a well-trained decision network is stored in the RSU for assisting in the vehicular lane-changing decisions. Thus, we can combine the realistic roadmap and vehicular density data with SUMO's vehicle-following and safety control simulators, and thus create the DT for simulating and predicting the vehicle speed and position within a certain time slots. The predicted vehicle speed and position can be utilized to calculate the TTC value Π_i^t.

B. Performance Evaluation and Comparison

We conduct 1000 simulation periods (each simulation period corresponding to 1 second), where the vehicle positions, channel conditions and network control schemes are updated in each period. Three RSUs are set at the points of 250 meters, 500 meters and 750 meters alongside the road. We randomly select 10 vehicles as the investigated vehicles with task offloading requirements, while the other vehicles are considered as the background traffic flow. Each vehicle is assigned with 10 non-URLLC tasks. Each non-URLLC task is modeled as Poisson arrival process with 0.1 Mbits/s average arrival rate. In addition, the URLLC tasks of vehicular safety control applications are considered. Different from the non-URLLC tasks, the URLLC tasks are generated based on DT's vehicular safety prediction results by satisfying $\Pi_i^t < \overline{\Pi}$. $\overline{\Pi}$ is the TTC safety threshold, which can be set as 1s, 3s and 6s in our simulation. In other words, only when $\Pi_i^t < \overline{\Pi}$ (which means that the vehicular safety condition is tense), the URLLC tasks of safety control applications are generated. For each vehicle, 10 URLLC tasks are generated, and each task is modeled as Poisson arrival process with 0.1 Mbits/s average arrival rate. The channel bandwidth is 5 MHz. The channel model utilizes Rayleigh fading. For the purpose of comparing the performance of our proposed scheme, the following two benchmarks are considered:

- **Scheme of Non-Robust Optimization (SNRO):** This scheme leverages DT prediction results to perform joint resource reservation and task offloading, but ignores robust optimization for handling the DT prediction inaccuracy [34]. Hence, the prediction error can result in either over or under utilization of communication and computation resources.
- **Scheme of Conventional Setup (SCS):** This scheme performs task offloading without DT, and thus channel and computation resources cannot be reserved for the URLLC tasks [42]. Hence, the URLLC task offloading priority to access channel and computation resources are not guaranteed. And the task offloading is based on the computation and communication rate maximization.

C. Resource Reservation Results

Fig. 3 illustrates the reserved number of channel and computation resources versus varying Γ_i with three different levels of TTC safey threshold $\overline{\Pi}$, respectively. Under the same level of uncertainty Γ_i, the smaller the TTC safety threshold $\overline{\Pi}$, the more channel and computation resources are reserved for each URLLC task. The reason is that less URLLC tasks are triggered for smaller $\overline{\Pi}$ and thus each task is able to utilize more resources. It can be also observed that the number of reserved channel and computation resources gradually rises, which can reach the maximum value due to the overall resource limitation, as Γ_i increases. The reason is that the number of uncertain constraints which are handled by the proposed solution in the resource reservation problem gradually increases as Γ_i increases. The increasing uncertainty requires more channel and computation resources to be reserved and then allocated for handling the increasing problem constraint uncertainty.

D. Algorithm Convergence

Fig. 4 demonstrates the cumulative number of matched channel resources and computation resources of the chan-

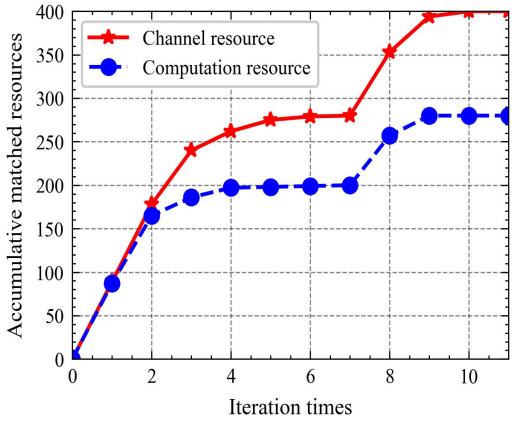

Fig. 4. Accumulative matched resources versus algorithm iteration times.

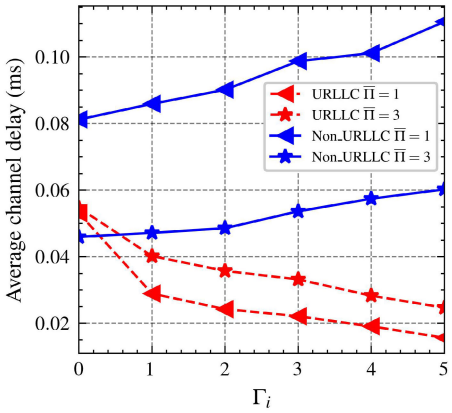

(a) Channel resources

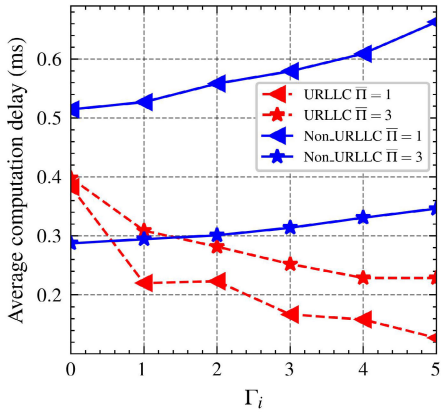

(b) Computation resources

Fig. 5. Average channel and computation delays versus Γ_i.

nel and computation resource matching algorithms (i.e., **Algorithm 1, Algorithm 2**), respectively. The first 7 iterations demonstrate the resource matching of the URLLC tasks, which starts to converge at about the 4th iteration. After all the URLLC tasks are matched successfully, the matching for non-URLLC tasks begins, which takes about 3 iteration times to converge.

E. Communication and Computation Delay

Figs. 5 a and b present the average communication and computation delay versus varying Γ_i for the URLLC and non-URLLC tasks with $\overline{\Pi}=1$ and $\overline{\Pi}=3$, respectively. Given the same level of uncertainty, as more extra channel resources are allocated for each URLLC tasks for smaller $\overline{\Pi}$, the average communication delay for URLLC tasks is slightly lower while the average delay for non-URLLC tasks is much higher. It can also be observed that the average communication delay of the URLLC tasks significantly decreases with the increasing Γ_i. On the contrary, the average communication delay of the non-URLLC task increases. The reason is that as the level of conservatism in the resource reservation problem increases, more channels are determined to be reserved for the URLLC tasks. Since the overall computation resource is limited, the available channels for the non-URLLC tasks are reduced, leading to increased communication delay. We can observe the same tendency for the computation delay in Fig. 5b.

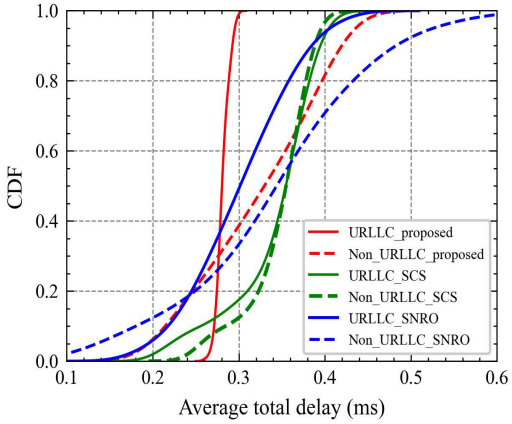

Fig. 6. CDF curves of average task delay under different schemes.

F. Task Delay Comparison

In this part, we compare the average total delay of our proposed scheme with the SNRO and SCS benchmarks, where cumulative distribution functions (CDF) of the average total delay are presented in Fig. 6. It can be observed that the URLLC task offloading delay is 0.27 ms (proposed), 0.30 ms (SNRO) and 0.35 ms (SCS) when CDF=0.5. The reason is that the proposed method can use the DT prediction results to satisfy the URLLC delay requirements. The SNRO cannot handle the DT prediction error efficiently, which leads to larger URLLC delay. In addition, the URLLC task delay of the SNRO scheme distributes more widely than our proposed scheme. The reason is due to its low robustness for handling the DT prediction error. The SCS shows minimal performance difference between the URLLC and non-URLLC tasks, which means that the URLLC delay cannot be efficiently guaranteed.

G. Task Delay Versus Varying DT Prediction Error

In Fig. 7, the effects of different DT prediction error on the URLLC task delay are compared between our proposed scheme and the SNRO scheme. Without loss of generality, we utilize $\hat{C}$ to represent the channel resource requirement prediction error. And larger $\hat{C}$ value means larger DT prediction error. We can observe that as $\hat{C}$ increases, the performance of the SNRO scheme fluctuates frequently while

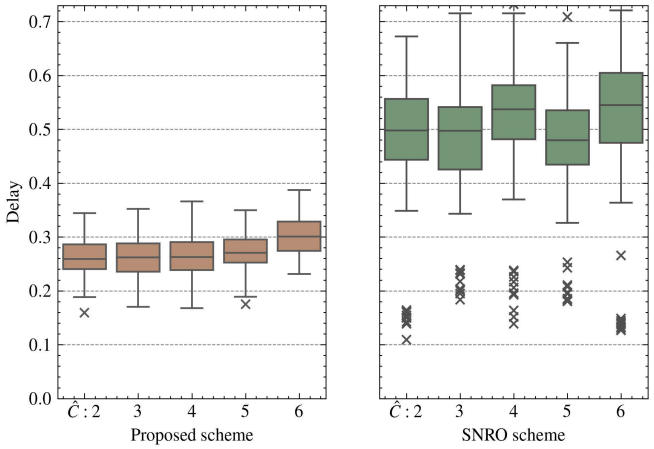

Fig. 7. URLLC task delay versus DT prediction error $\hat{C}$ under different schemes.

our proposed scheme shows better stability. The reason is that our proposed robust optimization balances the tradeoff between the optimization objective optimality and the prediction error. Thus, a more stable solution can be obtained by adjusting the tradeoff parameter Γ_i. By contrast, the SNRO utilize the inaccurate constraints with prediction error for resource reservation, for instance, the ranges between $C+\hat{C}$ and $C-\hat{C}$. Thus, the solutions are subject to the prediction error, which show instability.

VIII. Conclusion

In this paper, we present a DT empowered MEC framework for C-V2X communications, which jointly optimizes the resource reservation and the task offloading with mixed URLLC and non-URLLC tasks. The physical domain and the DT domain of proposed C-V2X framework are elaborated, respectively. The resource reservation problem, which resides in the DT domain, is firstly formulated and solved by a robust optimization approach, and the optimized reserved number of channel and computation resources are found by adjusting the robust parameter. The task offloading problem, which resides in the physical domain, is based on the output of optimized resource reservation solutions. And matching theory is leveraged to solve the task offloading problem. In the simulation, we construct a SUMO based DT simulator for capturing realistic road network features. Simulation results demonstrate that the proposed task offloading scheme can significantly reduce the average URLLC task and shows better stability compared against the existing benchmarks.

Appendix I
Proof of Equivalence between Eq. (1) and Eq. (5)

Our aim is to transform the division coefficient $\frac{1}{\tilde{C}^t_{i,j}}, \frac{1}{\tilde{Q}^t_{i,j}}$ in C3, C4 of (1) into the multiplication coefficient $\tilde{A}^t_{i,j}$, $\tilde{B}^t_{i,j}$ in C3', C4' of (5). We now prove that C3 and C4 are equivalent to C3' and C4' in the following two steps.

- First, consider when $j \notin \mathcal{U}$ (accurate DT prediction results), $\widehat{C}^t_{i,j} = \widehat{Q}^t_{i,j} = 0$ and we have $\tilde{C}^t_{i,j} = C^t_{i,j}, \tilde{Q}^t_{i,j} = Q^t_{i,j}$. By substituting $\widehat{C}^t_{i,j} = \widehat{Q}^t_{i,j} = 0$ into the following equations, we have $\tilde{A}^t_{i,j} = \frac{1}{C^t_{i,j}} = \frac{1}{\tilde{C}^t_{i,j}}$, $\tilde{B}^t_{i,j} = \frac{1}{Q^t_{i,j}} = \frac{1}{\tilde{Q}^t_{i,j}}$.
- Second, consider when $j \in \mathcal{U}$ (inaccurate DT prediction results), $\tilde{C}^t_{i,j}, \tilde{Q}^t_{i,j}$ have uncertain values in the range of $\left[C^t_{i,j} - \widehat{C}^t_{i,j}, C^t_{i,j} + \widehat{C}^t_{i,j}\right]$, $\left[Q^t_{i,j} - \widehat{Q}^t_{i,j}, Q^t_{i,j} + \widehat{Q}^t_{i,j}\right]$. According to Eq. (6), we have $\tilde{A}^t_{i,j} + \widehat{A}^t_{i,j} = \frac{1}{C^t_{i,j} - \widehat{C}^t_{i,j}}$ and $\tilde{A}^t_{i,j} - \widehat{A}^t_{i,j} = \frac{1}{C^t_{i,j} + \widehat{C}^t_{i,j}}$, $\tilde{B}^t_{i,j} + \widehat{B}^t_{i,j} = \frac{1}{Q^t_{i,j} - \widehat{Q}^t_{i,j}}$, $\tilde{B}^t_{i,j} - \widehat{B}^t_{i,j} = \frac{1}{Q^t_{i,j} + \widehat{Q}^t_{i,j}}$. Thus, we can obtain that the uncertain ranges $\left[\tilde{A}^t_{i,j} - \widehat{A}^t_{i,j}, \tilde{A}^t_{i,j} + \widehat{A}^t_{i,j}\right]$, $\left[\tilde{B}^t_{i,j} - \widehat{B}^t_{i,j}, \tilde{B}^t_{i,j} + \widehat{B}^t_{i,j}\right]$ in C3' and C4' correspond to $\left[\frac{1}{C^t_{i,j} + \widehat{C}^t_{i,j}}, \frac{1}{C^t_{i,j} - \widehat{C}^t_{i,j}}\right]$, $\left[\frac{1}{Q^t_{i,j} + \widehat{Q}^t_{i,j}}, \frac{1}{Q^t_{i,j} - \widehat{Q}^t_{i,j}}\right]$ in C3 and C4.

Appendix II
Proof of Proposition 2

We now prove *Proposition 2*, i.e., the violation probability of the ith sub-constraint of C3' as follows:

$$
\begin{aligned}
&\mathrm{P_r}\left\{\sum_{j\in\mathcal{J}_{\mathrm{UR}}} \tilde{A}^t_{i,j}x^*_j < \Psi^1_i\right\}\\
&= \mathrm{P_r}\left\{\sum_{j\in\mathcal{J}_{\mathrm{UR}}} A^t_{i,j}x^*_j + \sum_{j\in\mathcal{U}_i} \eta_{i,j}\widehat{A}^t_{i,j}x^*_j < \Psi^1_i\right\}\\
&\le \mathrm{P_r}\left\{\sum_{j\in\mathcal{U}_i} \eta_{i,j}\widehat{A}^t_{i,j}x^*_j < \sum_{j\in\mathcal{S}^*_i} \widehat{A}^t_{i,j}x^*_j + (\Gamma_i - \lfloor\Gamma_i\rfloor)\widehat{A}_{i,l^*_i}x^*_{l^*_i}\right\} \qquad \text{(B.1)}\\
&= \mathrm{P_r}\left\{\sum_{j\in\mathcal{U}_i/\mathcal{S}^*_i} \eta_{i,j}\widehat{A}^t_{i,j}x^*_j < \sum_{j\in\mathcal{S}^*_i} \widehat{A}^t_{i,j}x^*_j(1-\eta_{i,j})\right.\\
&\quad \left. + (\Gamma_i - \lfloor\Gamma_i\rfloor)\widehat{A}_{i,l^*_i}x^*_{l^*_i}\right\}\\
&\le \mathrm{P_r}\left\{\sum_{j\in\mathcal{U}_i/\mathcal{S}^*_i} \eta_{i,j}\widehat{A}^t_{i,j}x^*_j < \widehat{A}^t_{i,r^*}x^*_{r^*}\right.\\
&\quad \left.\left(\sum_{j\in\mathcal{S}^*_i}(1-\eta_{i,j}) + (\Gamma_i - \lfloor\Gamma_i\rfloor)\right)\right\} \qquad \text{(B.2)}\\
&= \mathrm{P_r}\left\{\sum_{j\in\mathcal{S}^*_i}\eta_{i,j} + \sum_{j\in\mathcal{U}_i/\mathcal{S}^*_i} \frac{\widehat{A}^t_{i,j}x^*_j}{\widehat{A}^t_{i,r^*}x^*_{r^*}}\eta_{i,j} < \Gamma_i\right\} \qquad \text{(B.3)}\\
&= \mathrm{P_r}\left\{\sum_{j\in\mathcal{U}_i}\gamma_{i,j}\eta_{i,j} < \Gamma_i\right\}\\
&\le \mathrm{P_r}\left\{\sum_{j\in\mathcal{U}_i}\gamma_{i,j}\eta_{i,j} \le \Gamma_i\right\} \qquad \text{(B.4)}
\end{aligned}
$$

Inequality (B.1) is derived by substituting the optimal x^*_j into Eq. (9), and relaxing the 'maximization' of (9), and relaxing the subtraction into the addition. Based on the above

operations, we can obtain the following equation:

$$\sum_{j\in\mathcal{J}_{\mathrm{UR}}} A^t_{i,j}x^*_j + \left(\sum_{j\in\mathcal{S}^*_i} \widehat{A}^t_{i,j}x^*_j + (\Gamma_i - \lfloor\Gamma_i\rfloor)\widehat{A}_{i,l^*_i}x^*_{l^*_i}\right) \geq \Psi^1_i$$

which can be further derived as:

$$\Psi^1_i - \sum_{j\in\mathcal{J}_{\mathrm{UR}}} A^t_{i,j}x^*_j \leq \sum_{j\in\mathcal{S}^*_i} \widehat{A}^t_{i,j}x^*_j + (\Gamma_i - \lfloor\Gamma_i\rfloor)\widehat{A}_{i,l^*_i}x^*_{l^*_i}$$

Inequality (B.2) is based on $1-\eta_{i,j} \geq 0$ and $r^* = \arg\max_{r\in\mathcal{S}^*_i\cup\{l^*_i\}} \hat{A}_{i,r}x^*_r$.

Transformation from (B.3) to (B.4) is based on the definition of $\gamma_{i,j}$.

To this end, we can prove that $\mathrm{P_r}\left\{\sum_{j\in\mathcal{J}_{\mathrm{UR}}} \widetilde{A}^t_{i,j}x^*_j < \Psi^1_i\right\} \leq \mathrm{P_r}\left\{\sum_{j\in\mathcal{U}_i} \gamma_{i,j}\eta_{i,j} \leq \Gamma_i\right\}$.

REFERENCES

[1] Y. Fu, C. Li, F. R. Yu, T. H. Luan, and Y. Zhang, "A selective federated reinforcement learning strategy for autonomous driving," *IEEE Trans. Intell. Transp. Syst.*, vol. 24, no. 2, pp. 1655–1668, Feb. 2023, doi: 10.1109/TITS.2022.3219644.

[2] J. Zhang and K. B. Letaief, "Mobile edge intelligence and computing for the Internet of Vehicles," *Proc. IEEE*, vol. 108, no. 2, pp. 246–261, Feb. 2020.

[3] T. Zhang, J. Xue, Y. Xu, K. Yu, and H. Zhou, "Dynamic radio resource slicing for service-oriented 5G/B5G C-V2X networks," in *Proc. IEEE/CIC Int. Conf. Commun. China (ICCC)*, Aug. 2022, pp. 1095–1100.

[4] W. Duan, J. Gu, M. Wen, G. Zhang, Y. Ji, and S. Mumtaz, "Emerging technologies for 5G-IoV networks: Applications, trends and opportunities," *IEEE Netw.*, vol. 34, no. 5, pp. 283–289, Sep. 2020.

[5] J. Chen, H. Wu, P. Yang, F. Lyu, and X. Shen, "Cooperative edge caching with location-based and popular contents for vehicular networks," *IEEE Trans. Veh. Technol.*, vol. 69, no. 9, pp. 10291–10305, Sep. 2020.

[6] R. Liu et al., "ROS-based collaborative driving framework in autonomous vehicular networks," *IEEE Trans. Veh. Technol.*, vol. 72, no. 6, pp. 6987–6999, Jun. 2023.

[7] H. Liang et al., "A dynamic resource allocation model based on SMDP and DRL algorithm for truck platoon in vehicle network," *IEEE Internet Things J.*, vol. 9, no. 12, pp. 10295–10305, Jun. 2022.

[8] N. Cheng et al., "Space/aerial-assisted computing offloading for IoT applications: A learning-based approach," *IEEE J. Sel. Areas Commun.*, vol. 37, no. 5, pp. 1117–1129, May 2019.

[9] Q. Wang, J. Wan, and X. Li, "Robust hierarchical deep learning for vehicular management," *IEEE Trans. Veh. Technol.*, vol. 68, no. 5, pp. 4148–4156, May 2019.

[10] M. Grieves and J. Vickers, "Digital twin: Mitigating unpredictable, undesirable emergent behavior in complex systems," in *Transdisciplinary Perspectives on Complex Systems: New Findings and Approaches*. Cham, Switzerland: Springer, 2017.

[11] M. Shafto et al., "Modeling, simulation, information technology & processing roadmap," *Nat. Aeronaut. Space Admin.*, vol. 32, pp. 1–38, Sep. 2012.

[12] F. Tang, X. Chen, T. K. Rodrigues, M. Zhao, and N. Kato, "Survey on digital twin edge networks (DITEN) toward 6G," *IEEE Open J. Commun. Soc.*, vol. 3, pp. 1360–1381, 2022.

[13] P. A. Lopez et al., "Microscopic traffic simulation using SUMO," in *Proc. 21st Int. Conf. Intell. Transp. Syst. (ITSC)*, Nov. 2018, pp. 2575–2582.

[14] J. Gao, Z. Kuang, J. Gao, and L. Zhao, "Joint offloading scheduling and resource allocation in vehicular edge computing: A two layer solution," *IEEE Trans. Veh. Technol.*, vol. 72, no. 3, pp. 3999–4009, Mar. 2023.

[15] T. D. T. Nguyen, V. Nguyen, V.-N. Pham, L. N. T. Huynh, M. D. Hossain, and E.-N. Huh, "Modeling data redundancy and cost-aware task allocation in MEC-enabled Internet-of-Vehicles applications," *IEEE Internet Things J.*, vol. 8, no. 3, pp. 1687–1701, Feb. 2021.

[16] X. Hou et al., "Reliable computation offloading for edge-computing-enabled software-defined IoV," *IEEE Internet Things J.*, vol. 7, no. 8, pp. 7097–7111, Aug. 2020.

[17] G. Wang and F. Xu, "Regional intelligent resource allocation in mobile edge computing based vehicular network," *IEEE Access*, vol. 8, pp. 7173–7182, 2020.

[18] Y. Sun, S. Zhou, and Z. Niu, "Distributed task replication for vehicular edge computing: Performance analysis and learning-based algorithm," *IEEE Trans. Wireless Commun.*, vol. 20, no. 2, pp. 1138–1151, Feb. 2021.

[19] Y. Cui, L. Du, H. Wang, D. Wu, and R. Wang, "Reinforcement learning for joint optimization of communication and computation in vehicular networks," *IEEE Trans. Veh. Technol.*, vol. 70, no. 12, pp. 13062–13072, Dec. 2021.

[20] X. Chen, C. Wu, Z. Liu, N. Zhang, and Y. Ji, "Computation offloading in beyond 5G networks: A distributed learning framework and applications," *IEEE Wireless Commun.*, vol. 28, no. 2, pp. 56–62, Apr. 2021.

[21] S. Tian, C. Chang, S. Long, S. Oh, Z. Li, and J. Long, "User preference-based hierarchical offloading for collaborative cloud-edge computing," *IEEE Trans. Services Comput.*, vol. 16, no. 1, pp. 684–697, Jan. 2023.

[22] Z. Ning, J. Huang, X. Wang, J. J. P. C. Rodrigues, and L. Guo, "Mobile edge computing-enabled Internet of Vehicles: Toward energy-efficient scheduling," *IEEE Netw.*, vol. 33, no. 5, pp. 198–205, Sep. 2019.

[23] Y. Zhai et al., "An energy aware offloading scheme for interdependent applications in software-defined IoV with fog computing architecture," *IEEE Trans. Intell. Transp. Syst.*, vol. 22, no. 6, pp. 3813–3823, Jun. 2021.

[24] W. Bao, C. Wu, S. Guleng, J. Zhang, K. A. Yau, and Y. Ji, "Edge computing-based joint client selection and networking scheme for federated learning in vehicular IoT," *China Commun.*, vol. 18, no. 6, pp. 39–52, Jun. 2021.

[25] Y. Liu et al., "Physical layer security assisted computation offloading in intelligently connected vehicle networks," *IEEE Trans. Wireless Commun.*, vol. 20, no. 6, pp. 3555–3570, Jun. 2021.

[26] T. Xiao, C. Chen, and S. Wan, "Mobile-edge-platooning cloud: A lightweight cloud in vehicular networks," *IEEE Wireless Commun.*, vol. 29, no. 3, pp. 87–94, Jun. 2022.

[27] C. Hu et al., "Digital twin-assisted real-time traffic data prediction method for 5G-enabled Internet of Vehicles," *IEEE Trans. Ind. Informat.*, vol. 18, no. 4, pp. 2811–2819, Apr. 2022.

[28] X. Liao et al., "Cooperative ramp merging design and field implementation: A digital twin approach based on vehicle-to-cloud communication," *IEEE Trans. Intell. Transp. Syst.*, vol. 23, no. 5, pp. 4490–4500, May 2022.

[29] C. Tan, X. Li, T. H. Luan, B. Gu, Y. Qu, and L. Gao, "Digital twin based remote resource sharing in Internet of Vehicles using consortium blockchain," in *Proc. IEEE 94th Veh. Technol. Conf. (VTC2021-Fall)*, Aug. 2021, pp. 1–6.

[30] L. Zhao, G. Han, Z. Li, and L. Shu, "Intelligent digital twin-based software-defined vehicular networks," *IEEE Netw.*, vol. 34, no. 5, pp. 178–184, Sep. 2020.

[31] W. Sun, H. Zhang, R. Wang, and Y. Zhang, "Reducing offloading latency for digital twin edge networks in 6G," *IEEE Trans. Veh. Technol.*, vol. 69, no. 10, pp. 12240–12251, Oct. 2020.

[32] X. Xu et al., "Service offloading with deep Q-network for digital twinning-empowered Internet of Vehicles in edge computing," *IEEE Trans. Ind. Informat.*, vol. 18, no. 2, pp. 1414–1423, Feb. 2022.

[33] N. Cha, C. Wu, T. Yoshinaga, Y. Ji, and K. A. Yau, "Virtual edge: Exploring computation offloading in collaborative vehicular edge computing," *IEEE Access*, vol. 9, pp. 37739–37751, 2021.

[34] K. Zhang, J. Cao, S. Maharjan, and Y. Zhang, "Digital twin empowered content caching in social-aware vehicular edge networks," *IEEE Trans. Computat. Social Syst.*, vol. 9, no. 1, pp. 239–251, Feb. 2022.

[35] B. Fan, Y. Wu, Z. He, Y. Chen, T. Q. S. Quek, and C. Xu, "Digital twin empowered mobile edge computing for intelligent vehicular lane-changing," *IEEE Netw.*, vol. 35, no. 6, pp. 194–201, Nov. 2021.

[36] M. Sim, "Robust optimization," Ph.D. dissertation, Massachusetts Inst. Technol., Cambridge, MA, USA, 2004.

[37] D. Bertsimas and M. Sim, "The price of robustness," *Oper. Res.*, vol. 52, no. 1, pp. 35–53, 2004.

[38] R. Lorentzen and R. Nilsen, "Application of linear programming to the optimal difference triangle set problem," *IEEE Trans. Inf. Theory*, vol. 37, no. 5, pp. 1486–1488, Sep. 1991.

[39] Y. Gu, W. Saad, M. Bennis, M. Debbah, and Z. Han, "Matching theory for future wireless networks: Fundamentals and applications," *IEEE Commun. Mag.*, vol. 53, no. 5, pp. 52–59, May 2015.

[40] R. Martínez, J. Massó, A. Neme, and J. Oviedo, "On group strategy-proof mechanisms for a many-to-one matching model," *Int. J. Games Theory*, vol. 33, no. 1, pp. 115–128, Dec. 2004.

[41] A. Kesting, M. Treiber, and D. Helbing, "Enhanced intelligent driver model to access the impact of driving strategies on traffic capacity," *Philosophical Trans. Roy. Soc. A, Math., Phys. Eng. Sci.*, vol. 368, no. 1928, pp. 4585–4605, Oct. 2010.

[42] X. Huang, R. Yu, S. Xie, and Y. Zhang, "Task-container matching game for computation offloading in vehicular edge computing and networks," *IEEE Trans. Intell. Transp. Syst.*, vol. 22, no. 10, pp. 6242–6255, Oct. 2021.

Bo Fan received the Ph.D. degree from the School of Information and Communications Engineering, Beijing University of Posts and Telecommunications (BUPT), Beijing, China, in 2018. From 2016 to 2017, he was with the Software Group, ETH Zürich, as a Visiting Scholar. He is currently an Associate Professor with the College of Metropolitan Transportation, Beijing University of Technology. His research interests include vehicular communication, visible light communication, and wireless resource management. He served as a TPC Member for IEEE VTC and ICCC; and a reviewer for IEEE WCNC, IEEE JOURNAL ON SELECTED AREAS IN COMMUNICATIONS, IEEE TRANSACTIONS ON INTELLIGENT TRANSPORTATION SYSTEMS, IEEE TRANSACTIONS ON WIRELESS COMMUNICATIONS, and IEEE TRANSACTIONS ON VEHICULAR TECHNOLOGY.

Zhenlin Xu is currently pursuing the M.Sc. degree in transport, infrastructure and logistics with Delft University of Technology, The Netherlands. He is also a Research Assistant with the Mobility of eXtended Reality (MXR) Laboratory and the Automated Driving and Simulation (ADaS) Laboratory, Delft University of Technology.

Zhidu Li (Senior Member, IEEE) received the PhD. degree in information and communications engineering from Beijing University of Posts and Telecommunications in 2018. He is currently a Professor with Chongqing University of Posts and Telecommunications. His research interests include network optimization and edge intelligence. He was a recipient of four Best Paper Awards from conferences, such as IEEE WCSP and IEEE BLOCKCHAIN.

Yuan Wu (Senior Member, IEEE) received the Ph.D. degree in electronic and computer engineering from The Hong Kong University of Science and Technology, Hong Kong, in 2010. He is currently an Associate Professor with the State Key Laboratory of Internet of Things for Smart City, University of Macau, Macau, China, and also with the Department of Computer and Information Science, University of Macau. His research interests include resource management for wireless networks, edge computing and edge intelligence, and green communications and computing. He was a recipient of the Best Paper Award from the IEEE ICC'2016, IEEE TCGCC'2017, IWCMC'2021, and IEEE WCNC'2023. He is on the editorial board of IEEE TRANSACTIONS ON VEHICULAR TECHNOLOGY, IEEE TRANSACTIONS ON NETWORK SCIENCE AND ENGINEERING, and IEEE INTERNET OF THINGS JOURNAL.

Yan Zhang (Fellow, IEEE) received the Ph.D. degree from the School of Electrical and Electronics Engineering, Nanyang Technological University, Singapore. He is currently a Full Professor with the Department of Informatics, University of Oslo, Oslo, Norway. His research interests include next generation wireless networks leading to 5G and cyber-physical systems. He is a fellow of IET; and an Elected Member of the Academia Europaea, the Royal Norwegian Society of Sciences and Letters (DKNVS), and Norwegian Academy of Technological Sciences. He is an editor of several IEEE publication.